Superior elasto-optic tetragonal SrTiO₃ films

M. Tyunina, N. Nepomniashchaia, V. Vetokhina, et al.

View Online   Export Citation   CrossMark

ARTICLES YOU MAY BE INTERESTED IN

Emerging materials for spin–charge interconversion
APL Materials 9, 120401 (2021); https://doi.org/10.1063/5.0076924

A growth diagram for chemical beam epitaxy of $GaP_{1-x}N_x$ alloys on nominally (001)-oriented GaP-on-Si substrates
APL Materials 9, 121101 (2021); https://doi.org/10.1063/5.0067209

Density dependent local structures in InTe phase-change materials
APL Materials 9, 121105 (2021); https://doi.org/10.1063/5.0073400

APL Materials

SPECIAL TOPIC: Emerging Materials for Spin-Charge Interconversion

Read Now!

Superior elasto-optic tetragonal SrTiO₃ films

View Online   Export Citation   CrossMark

M. Tyunina,[1,2,a] [ID] **N. Nepomniashchaia,**[2] [ID] **V. Vetokhina,**[2] [ID] and **A. Dejneka**[2] [ID]

AFFILIATIONS

[1] Microelectronics Research Unit, Faculty of Information Technology and Electrical Engineering, University of Oulu, P.O. Box 4500, FI-90014 Oulu, Finland
[2] Institute of Physics of the Czech Academy of Sciences, Na Slovance 2, 18221 Prague, Czech Republic

[a] Author to whom correspondence should be addressed: marina.tjunina@oulu.fi

ABSTRACT

Cutting-edge acousto-optic devices require optically transparent thin films, which possess a high index of refraction and large elasto-optic coefficients. For the wide near-infrared to ultraviolet spectral region, the mainstream technology employs lithium niobate crystals, which interferes with the vital demands of global sustainability. Here, we demonstrate unprecedented elasto-optic properties in thin films of sustainable and environmentally friendly strontium titanate [SrTiO₃ (STO)]. Compared to cubic STO, a nearly twofold increase in elasto-optic coefficients is achieved in epitaxial tetragonal STO films, which concurrently exhibit excellent transparency and a high index of refraction at wavelengths from 400 to 1700 nm. The room-temperature non-polar state is evidenced by the thermo-optical behavior of the films. The obtained enhancement is related to the tetragonal antiferrodistortive phase of STO. It is suggested that such films can form a platform for future sustainable acousto-optic materials.

Controlling light propagation in solids by mechanical strain or an electric field constitutes the basis for a vast variety of modern optical devices.[1] A change in the index of refraction by strain, or the elasto-optic effect, enables important acousto-optic devices and applications.[2,3] The key parameters of a material for premium devices are both the high index of refraction and large elasto-optic coefficients in the material's transparency spectral range.[2] Because thin films allow for increased power density and a longer interaction length, thin-film devices possess significant advantages over their bulk counterparts.[2,4] Correspondingly, for the wide near-infrared (NIR) to ultraviolet (UV) spectral region, thin layers of lithium niobate [LiNbO₃ (LNO)] on insulating substrates (LNOI) empower present-day devices.[5–10] The LNOI structures are prepared by cutting LNO slices from bulk crystals, bonding the slices to low-index substrates, and final polishing. In addition to the related nonproductive and environmentally harmful waste of LNO, the constituent elements of LNO—Li and Nb—belong to the so-called critical elements, whose abundance on the Earth is very small, but the demand is growing. Furthermore, the presence of Nb in LNO has a strongly deleterious impact across all environmental indicators, which are considered today.[11] We note that the widely studied epitaxial LNO films[12] cannot resolve the environmental and sustainability issues of LNO. Here, we demonstrate an alternative route toward elasto-optic films using perovskite oxide SrTiO₃ (STO), which is free of these issues.

For STO, compared to LNO, the constituent Sr is 25 times more abundant than Li, whereas Ti is 445 times more abundant than Nb: it is the ninth most abundant element in the Earth's crust. Strontium is commonly present in natural minerals and food and is essential for life. Neither the biological role nor the environmental effects have been reported for titanium. The human body can tolerate Ti in large doses. Similar to LNO, STO is a wide bandgap material, ensuring high transparency in the NIR–UV range, where it possesses a high index of refraction. The maximal elasto-optic coefficients (for the wavelength 600 nm) are ~0.15 in STO and ~0.18 in LNO, suggesting that for some devices (e.g., modulators), STO crystals are nearly as well suited as LNO (Table S1 of the supplementary material). Importantly, in contrast to fundamental and technical difficulties in the synthesis of epitaxial LNO films,[12] perfect epitaxial films of STO have been grown on a variety of substrates, including commercial silicon ones.[13,14] A hypothetical epitaxial STO film, where the elasto-optic coefficient could be enhanced to ~0.3, would totally surpass LNO (Table S1 of the supplementary material). Here, we achieved such an enhancement using epitaxial stabilization of a non-polar tetragonal antiferrodistortive (AFD) phase of STO.

In bulk unstressed STO crystals, the transition from the cubic paraelectric (PE) phase to the tetragonal AFD phase occurs on cooling at ~104 K. The PE–AFD transition was theoretically suggested to modify the electronic band structure and, consequently, optical properties of STO,[15,16] whereas negligibly small optical changes were experimentally detected in crystals.[17,18] However, the optical properties of the AFD phase can be markedly more sensitive to strain than those of the PE phase,[16] which can raise elasto-optic coefficients. Furthermore, in contrast to the low-temperature AFD phase in crystals, the high-temperature AFD phase can be stabilized in epitaxial films, grown on compressive substrates.[19–21] In this work, we verified the conceived possible advancement as follows.

Cube-on-cube-type epitaxial films of STO were grown on $(001)(La_{0.3}Sr_{0.7})(Al_{0.65}Ta_{0.35})O_3$ (LSAT) substrates, which impose biaxial compressive in-plane misfit strain and hence induce out-of-plane lattice elongation and tetragonality in the films. We note that LSAT substrates enable an in-plane lattice parameter of 3.868 Å, which is close to that of ~3.840 Å for STO on Si substrates. Therefore, our observations are relevant for potential commercial STO/Si films. The films were grown by pulsed laser deposition in oxygen ambience. The films were tetragonal perovskite, with the epitaxial relationship $(001)[100]STO||(001)[100]LSAT$ and a longer crystal axis normal to the substrate surface. By controlling gas pressure, the coherent films with thicknesses up to ~150 nm were obtained and the out-of-plane tensile strain was tuned from ~0.5 to ~1.7% (Table S2 of the supplementary material). The presence of oxygen vacancies facilitated coherency and raised the out-of-plane strain above the misfit level. The detailed analysis and multiscale modeling of the growth were presented in Ref. 22.

The optical properties of the films, reference STO crystal, and LSAT substrate were studied using variable angle spectroscopic ellipsometry. The bare LSAT single-crystal substrate was investigated to ensure accurate studies of the properties of the films. We used an epitaxially polished (001)-oriented single-crystal STO substrate (MTI Corp.) as the reference crystal. The measurements were performed on a Woollam vacuum ultraviolet (VUV) ellipsometer at room temperature, in dry nitrogen atmosphere, and at photon energies of (0.75–8.8) eV. The high-temperature measurements were performed in air at photon energies of (0.75–6.5) eV. The details of the measurements and data processing can be found in Refs. 23–25.

Typical examples of ellipsometric spectra and fitted data are given in Fig. S1 of the supplementary material.

The dielectric functions ($\varepsilon^* = \varepsilon_1 + i\varepsilon_2$) and optical constants (index of refraction n, extinction coefficient k, and absorption coefficient α) were determined as a function of wavelength (or photon energy) in the STO films and crystal (Fig. 1 and Figs. S2 and S3 of the supplementary material).

The films exhibit excellent transparency in the wavelength range of 400–1700 nm [Figs. 1(a) and 1(b) and Fig. S2 of the supplementary material]. Moreover, compared to the crystal, the absorption edge is shifted to shorter wavelengths in the films [Fig. 1(a)]. In the transparency spectral range, the index of refraction is large (>2.2) and depends on the strain in the films [Fig. 1(c)].

The elasto-optic behavior of the tetragonal STO/LSAT films can be described by[26–28]

$$\Delta(n_{11}^{-2}) = (p_{1111} + p_{1122})s_{11} + p_{1133}s_{33} \approx n^{-2} - n_0^{-2}. \quad (1)$$

Here, n_{11} and p_{1122}, p_{1122}, and p_{1133} are the index of refraction and the elasto-optic coefficients, respectively.[26–28] The biaxial in-plane strain is $s_a = s_{11}$, and the out-of-plane strain is $s_c = s_{33}$ correspondingly. As mentioned above, the AFD transition has no detectable effect on the index of refraction in the absence of strain.[17,18] Therefore, the index of refraction in the crystal, n_0, is used in (1). The index of refraction n is extracted from the ellipsometric data.

In agreement with expression (1), the experimentally determined refraction alterations $\Delta(n^{-2})$ increase linearly with the out-of-plane strain s_c [Fig. 2(a)]. The coefficients p_{1133} and (p_{1111} + p_{1122}) were determined from the linear fits for different wavelengths [Figs. 2(b) and 2(c)]. We emphasize that the extracted p_{1133} is insensitive to the choice of the reference n_0 in (1). The films possess a very large positive p_{1133} [Fig. 2(b)], whose magnitude exceeds those of p_{11} in bulk STO and p_{1133} in bulk LNO. The negative sign of the sum (p_{1111} + p_{1122}) in the films [Fig. 2(c)] is typical for tetragonal perovskite oxides.[27]

The coefficients p_{1133} and (p_{1111} + p_{1122}) bear a weak wavelength dispersion compared to that in crystals of LNO or STO.[28] The dispersion was analyzed using the phenomenological relationship,[28]

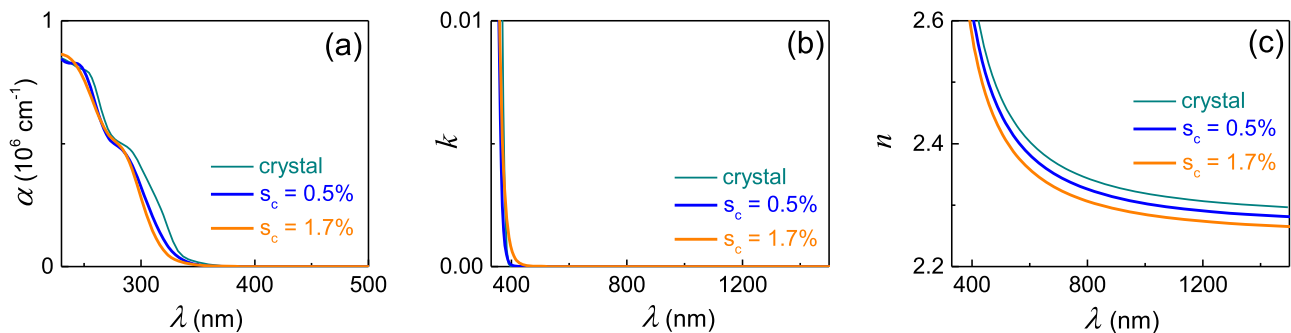$$p^* = |p| \cdot (1 - n^{-2})^{-2} = p_0^* + \kappa\lambda^{-2}, \quad (2)$$

FIG. 1. (a) Absorption coefficient, (b) extinction coefficient, and (c) index of refraction as a function of wavelength in the strained STO films. Data for the reference crystal are shown by thin curves.
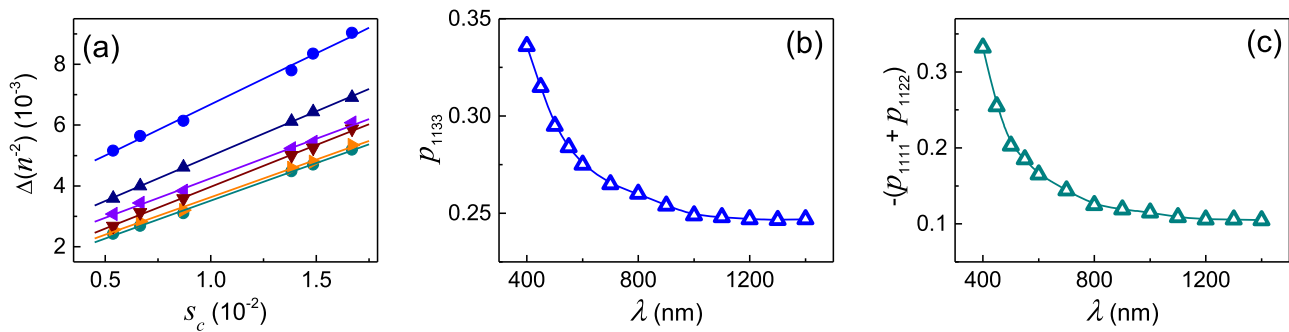
FIG. 2. (a) Refraction variations $\Delta(n^{-2})$ as a function of strain s_c at different wavelengths. Straight lines show fits. The wavelengths are 1200, 1000, 800, 600, 500, and 400 nm from the lower line up. (b) and (c) Elasto-optic coefficients (b) p_{1133} and (c) $-(p_{1111} + p_{1122})$ as a function of wavelength.

where p^* is the normalized elasto-optic coefficient and the dispersion constant κ is material-specific.[28] The linear relationships between p^* and λ^{-2} are valid for both $(p_{1133})^*$ and $(p_{1111} + p_{1122})^*$ in the AFD STO films (Fig. 3), similar to the linear dependences in bulk STO and LNO.[28] The dispersion constants were found from the linear fits in Fig. 3. In the STO films, the constant κ for the coefficient $(p_{1133})^*$ is $\sim 0.015 \times 10^{-12}$ m^2, which is two orders of magnitude smaller than that of $\sim 1.1 \times 10^{-12}$ m^2 in LNO.[28] The constant κ for the coefficients $(p_{1111} + p_{1122})^*$ is 0.04×10^{-12} m^2 in the tetragonal STO films. For comparison, the dispersion constant is $\sim 0.5 \times 10^{-12}$ m^2 in the STO crystal.[28]

The enhanced elasto-optic coefficients, which possess relatively weak wavelength dispersion, together with the large index of refraction and excellent transparency of the AFD STO films, affirm that such films can be competitive elasto-optic materials (Table I of the supplementary material).

We relate the obtained enhanced elasto-optic properties to the tetragonal non-polar AFD phase of STO. This phase is in perfect agreement with the up-to-date strain–temperature phase diagram of STO,[21] according to which our films are expected to experience a ferroelectric transition on cooling below ~ 200 K. However, to prove the room-temperature non-polar state in the films, we inspected their thermo-optical behavior, namely, the index of refraction as a function of temperature. For perovskite oxide ferroelectrics and the related crystals, it is well established that the appearance of

spontaneous crystal polarization manifests itself optically.[29–35] Specifically, the index of refraction in the transparency range exhibits a linear behavior $[n(T) \propto T]$ with the negative thermo-optical coefficient in non-polar phases of perovskite oxide ferroelectrics, whereas a deviation from such behavior signifies the presence of crystal polarization. The positive thermo-optical coefficient is typical for the ferroelectric state. The optical manifestations of polarization have also been experimentally confirmed both in thin films and in strain-induced ferroelectric transitions in epitaxial films.[36–38] Here, the absence of polarization is unambiguously demonstrated by the linear temperature dependence of the index of refraction $[n(T) \propto T]$: the negative slope of $n(T)$ in the films corresponds to that in the non-polar STO crystal (Fig. 4). We emphasize that the misfit-induced ferroelectric phase transition was clearly expressed by the change from the high-temperature negative thermo-optics $[n \propto T]$ to the low-temperature positive one in the strongly strained epitaxial films of STO as well as those of KTaO$_3$.[36] The thermo-optic behavior confirms the non-polar state of the strained tetragonal STO films studied here.

Explicit microscopic mechanisms of the phenomenal optical properties of the tetragonal AFD STO films are unknown. To get a preliminary insight into them, we examined the main optical interband transitions, which are manifested by the apparent lowest-energy and strongest critical point (CP) line at ~ 4.0 eV.[24] The second derivative of the dielectric function indicates a shift of this line to higher energies with an increase in strain (Fig. 5). This blueshift conforms to the theoretically shown strain-dependent widening of the optical gaps in the AFD phase.[16] Concurrently, according to the phenomenological model,[28] bandgap widening can drive the elasto-optic effect. Furthermore, in addition to the strain-stimulated bandgap behavior, electron–phonon coupling and phonon-related polarization oscillations can noticeably raise the elasto-optic coefficients in a non-polar phase of perovskite oxide ferroelectrics.[28] As found before, the presence of strong phonon effects is very likely in the tetragonal STO films.[24] These phonon effects and the related peculiar phonon hardening[39,40] in the non-polar AFD STO films await theoretical investigations.

In summary, for the broad spectral range (wavelengths of 400–1700 nm), large elasto-optic coefficients (up to ~ 0.3) in combination with high transparency and a large index of refraction (>2.2) were obtained in epitaxial tetragonal non-polar AFD films of STO.
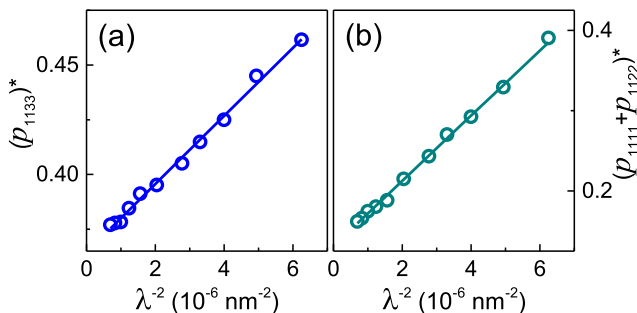

FIG. 3. Wavelength dispersion relationships for the normalized elasto-optic coefficients (a) $(p_{1133})^*$ and (b) $(p_{1111} + p_{1122})^*$. Straight lines show fits.
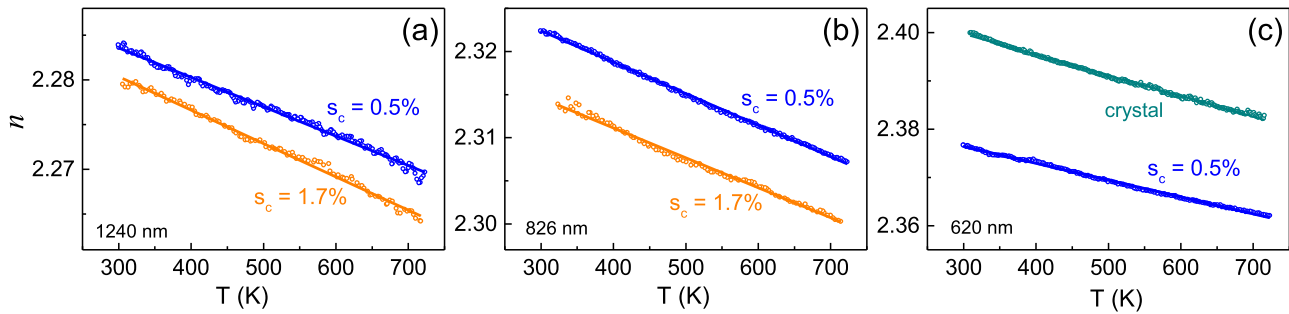
FIG. 4. Thermo-optical behavior: index of refraction as a function of temperature at different wavelengths of (a) 1240, (b) 826, and (c) 620 nm in the STO films (strain is marked on the plots) and crystal. Straight lines show fits.
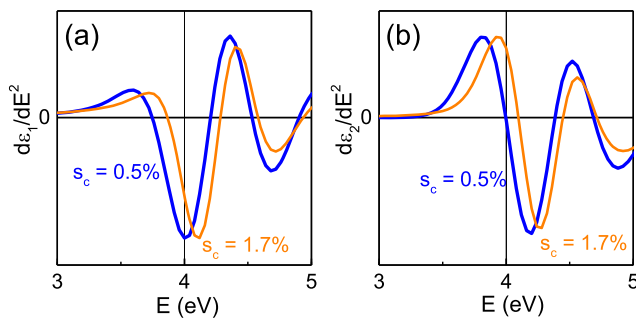

FIG. 5. Second derivatives of the (a) real and (b) imaginary parts of the dielectric function as a function of photon energy in the tetragonal STO films. The out-of-plane strain is marked on the plots.

Compared to cubic STO, the elasto-optic coefficients are significantly enhanced in the films, which was discussed in terms of the interband and phonon effects. Being environmentally friendly, sustainable, and compatible with silicon substrates, such STO films have a high potential for future acousto-optic materials.

See the supplementary material for elasto-optic figures of merit, list of samples, and ellipsometry data.

AUTHOR DECLARATIONS

Conflict of Interest

The authors have no conflicts to disclose.

DATA AVAILABILITY

The data that support the findings of this study are available from the corresponding author upon reasonable request.

REFERENCES

[1] *Handbook of Optics*, 2nd ed., edited by M. Bass (McGraw-Hill, New York, 1995).

[2] I. C. Chang, "Acousto-optic devices and applications," in *Handbook of Optics*, 2nd ed., edited by M. Bass (McGraw-Hill, New York, 1995), pp. 12.1–12.54.

[3] N. Savage, "Acousto-optic devices," Nat. Photonics **4**, 728 (2010).

[4] *Handbook of Optical Materials*, edited by M. J. Weber (CRC Press, Boca Raton, FL, 2003).

[5] L. Arizmendi, "Photonic applications of lithium niobate crystals," Phys. Status Solidi A **201**, 253 (2004).

[6] G. Poberaj, H. Hu, W. Sohler, and P. Günter, "Lithium niobate on insulator (LNOI) for micro-photonic devices," Laser Photonics Rev. **6**, 488 (2012).

[7] C. Wang *et al.*, "Integrated lithium niobate electro-optic modulators operating at CMOS-compatible voltages," Nature **562**, 101 (2018).

[8] A. Boes, B. Corcoran, L. Chang, J. Bowers, and A. Mitchell, "Status and potential of lithium niobate on insulator (LNOI) for photonic integrated circuits," Laser Photonics Rev. **12**, 1700256 (2018).

[9] M. He *et al.*, "High-performance hybrid silicon and lithium niobate Mach–Zehnder modulators for 100 Gbit s^{-1} and beyond," Nat. Photonics **13**, 359–364 (2019).

[10] Y. Qi and Y. Li, "Integrated lithium niobate photonics," Nanophotonics **9**, 1287 (2020).

[11] T. Ibn-Mohammed *et al.*, "Integrated hybrid life cycle assessment and supply chain environmental profile evaluations of lead based (lead zirconate titanate) versus lead-free (potassium sodium niobate) piezoelectric ceramics," Energy Environ. Sci. **9**, 3495 (2016).

[12] A. Bartasyte, S. Margueron, T. Baron, S. Oliveri, and P. Boulet, "Toward high-quality epitaxial LiNbO$_3$ and LiTaO$_3$ thin films for acoustic and optical applications," Adv. Mater. Interfaces **4**, 1600998 (2017).

[13] R. A. McKee, F. J. Walker, and M. F. Chisholm, "Crystalline oxides on silicon: The first five monolayers," Phys. Rev. Lett. **81**, 3014 (1998).

[14] S.-H. Baek and C.-B. Eom, "Epitaxial integration of perovskite-based multifunctional oxides on silicon," Acta Mater. **61**, 2734 (2013).

[15] E. Heifets, E. Kotomin, and V. A. Trepakov, "Calculations for antiferrodistortive phase of SrTiO$_3$ perovskite: Hybrid density functional study," J. Phys.: Condens. Matter **18**, 4845 (2006).

[16] R. F. Berger, C. J. Fennie, and J. B. Neaton, "Band gap and edge engineering via ferroic distortion and anisotropic strain: The case of SrTiO$_3$," Phys. Rev. Lett. **107**, 146804 (2011).

[17] V. Trepakov, A. Dejneka, P. Markovin, A. Lynnyk, and L. Jastrabik, "A 'soft electronic band' and the negative thermooptic effect in strontium titanate," New J. Phys. **11**, 083024 (2009).

[18] A. Dejneka, V. Trepakov, and L. Jastrabik, "Spectroscopic ellipsometry of SrTiO$_3$ crystals applied to antiferrodistortive surface phase transition," Phys. Status Solidi B **247**, 1951 (2010).

[19] N. A. Pertsev, A. K. Tagantsev, and N. Setter, "Phase transitions and strain-induced ferroelectricity in SrTiO$_3$ epitaxial thin films," Phys. Rev. B **61**, R825 (2000).

[20] Y. L. Li *et al.*, "Phase transitions and domain structures in strained pseudocubic (100) SrTiO₃ thin films," Phys. Rev. B **73**, 184112 (2006).

[21] T. Yamada, B. Wylie-van Eerd, O. Sakata, A. K. Tagantsev, H. Morioka, Y. Ehara, S. Yasui, H. Funakubo, T. Nagasaki, and H. J. Trodahl, "Phase transitions associated with competing order parameters in compressively strained SrTiO₃ thin films," Phys. Rev. B **91**, 214101 (2015).

[22] M. Tyunina, L. L. Rusevich, E. A. Kotomin, O. Pacherova, T. Kocourek, and A. Dejneka, "Epitaxial growth of perovskite oxide films facilitated by oxygen vacancies," J. Mater. Chem. C **9**, 1693 (2021).

[23] A. Dejneka, D. Chvostova, O. Pacherova, T. Kocourek, M. Jelinek, and M. Tyunina, "Optical effects induced by epitaxial tension in lead titanate," Appl. Phys. Lett. **112**, 031111 (2018).

[24] M. Tyunina, N. Nepomniashchaia, V. Vetokhina, and A. Dejneka, "Optics of epitaxial strained strontium titanate films," Appl. Phys. Lett. **117**, 082901 (2020).

[25] M. Tyunina, O. Vetokhina, N. Nepomniashchaia, O. Pacherova, S. Cichon, T. Kocourek, M. Jelinek, and A. Dejneka, "Multiple optical impacts of anion doping in epitaxial barium titanate films," APL Mater. **8**, 071107 (2020).

[26] A. Dejneka, M. Tyunina, J. Narkilahti, J. Levoska, D. Chvostova, L. Jastrabik, and V. A. Trepakov, "Tensile strain induced changes in the optical spectra of SrTiO₃ epitaxial thin films," Phys. Solid State **52**, 2082–2089 (2010).

[27] L. Chen, Y. Yang, Z. Gui, D. Sando, M. Bibes, X. K. Meng, and L. Bellaiche, "Large elasto-optic effect in epitaxial PbTiO₃ films," Phys. Rev. Lett. **115**, 267602 (2015).

[28] S. H. Wemple and M. DiDomenico, "Theory of the elasto-optic effect in nonmetallic crystals," Phys. Rev. B **1**, 193 (1970).

[29] W. J. Merz, "The electric and optical behavior of BaTiO₃ single-domain crystals," Phys. Rev. **76**, 1221 (1949).

[30] G. Burns and B. A. Scott, "Index of refraction in 'dirty' displacive ferroelectrics," Solid State Commun. **13**, 423 (1973).

[31] W. Kleemann, F. J. Schäfer, and M. D. Fontana, "Crystal optical studies of spontaneous and precursor polarization in KNbO₃," Phys. Rev. B **30**, 1148 (1984).

[32] W. Kleemann, F. J. Schäfer, and D. Rytz, "Crystal optical studies of precursor and spontaneous polarization in PbTiO₃," Phys. Rev. B **34**, 7873 (1986).

[33] O. Y. Korshunov, P. A. Markovin, and R. V. Pisarev, "Thermoopitical study of precursor polarization in ferroelectrics with diffuse phase transitions," Ferroelectr. Lett. **13**, 137 (1992).

[34] P. A. Markovin, W. Kleemann, R. Lindner, V. V. Lemanov, O. Y. Korshunov, and P. P. Syrnikov, "A crystal optical study of phase transitions in Sr₁₋ₓBaₓTiO₃ single crystals," J. Phys.: Condens. Matter **8**, 2377 (1996).

[35] M. Tyunina, A. Dejneka, D. Rytz, I. Gregora, F. Borodavka, M. Vondracek, and J. Honolka, "Ferroelectricity in antiferroelectric NaNbO₃ crystal," J. Phys.: Condens. Matter **26**, 125901 (2014).

[36] M. Tyunina, J. Narkilahti, M. Plekh, R. Oja, R. M. Nieminen, A. Dejneka, and V. Trepakov, "Evidence for strain-induced ferroelectric order in epitaxial thin-film KTaO₃," Phys. Rev. Lett. **104**, 227601 (2010).

[37] M. Tyunina, A. Dejneka, D. Chvostova, J. Levoska, M. Plekh, and L. Jastrabik, "Phase transitions in ferroelectric Pb₀.₅Sr₀.₅TiO₃ films probed by spectroscopic ellipsometry," Phys. Rev. B **86**, 224105 (2012).

[38] O. Pacherova, D. Chvostova, T. Kocourek, M. Jelinek, A. Dejneka, E. Eliseev, A. Morozovska, and M. Tyunina, "Thermooptical evidence of carrier-stabilized ferroelectricity in ultrathin electrodeless films," Sci. Rep. **8**, 8497 (2018).

[39] D. Nuzhnyy, J. Petzelt, S. Kamba, X. Martí, T. Čechal, C. M. Brooks, and D. G. Schlom, "Infrared phonon spectroscopy of a compressively strained (001) SrTiO₃ film grown on a (110) NdGaO₃ substrate," J. Phys.: Condens. Matter **23**, 045901 (2011).

[40] P. Marsik, K. Sen, J. Khmaladze, M. Yazdi-Rizi, B. P. P. Mallett, and C. Bernhard, "Terahertz ellipsometry study of the soft mode behavior in ultrathin SrTiO₃ films," Appl. Phys. Lett. **108**, 052901 (2016).